

Chapter 5 Control of Chaotic Attitude Motion

Abstract This chapter covers the control of chaos. It begins with an introduction to control of chaos. The control problem is formulated in the framework of system theory. The OGY method is presented as a significant and representative approach. Synchronization of chaos is briefly introduced. The parametric open-plus-closed-loop method and the stability criterion method are respectively proposed with the main ideas, the control laws, and the numerical examples. The chapter ends with controlling chaotic attitude motion. After the survey of recent investigations, planar libration of magnetic rigid spacecraft in an elliptic orbit in the gravitational and the magnetic field is treated as an example to demonstrate the applications of the parametric open-plus-closed-loop method and the stability criterion method.

Keywords control of chaos, system theory, synchronization of chaos, parametric open-plus-closed-loop method, stability criterion method, planar libration, magnetic rigid spacecraft, elliptic orbit

This chapter covers control of chaos. It begins with an introduction to control of chaos. The control problem is formulated in the framework of system theory. The OGY method is presented as a significant and representative approach. Synchronization of chaos is briefly introduced. The parametric open-plus-closed-loop method and the stability criterion method are respectively proposed with the main ideas, the control laws, and the numerical examples. The chapter ends with controlling chaotic attitude motion. After the survey of recent investigations, planar libration of magnetic rigid spacecraft in an elliptic orbit in the gravitational and the magnetic field is treated as an example to demonstrate the applications of the parametric open-plus-closed-loop method and the stability criterion method.

5.1 Control of Chaos: An Overview

5.1.1 Introduction

Chaos occurs in a large variety of engineering systems and natural processes. Identification and prediction of chaos is surely beneficial to scientific understanding

and technical applications, but chaos has to be controlled so that the benefits will be maximized. Traditionally, chaos is believed to be uncontrollable because any small disturbance usually leads to other chaotic motions but not to any regular motion. However, the pioneering work of Ott, Grebogi, and Yorke in 1990 demonstrated that chaos can be converted to any one of a large number of periodic motions by making only small perturbations of an available system parameter [1]. The contributions by Ott, Grebogi, and Yorke referred to as the **OGY method**, and its generalization will be presented in 5.1.3. Since then, controlling chaos has been one of the most fascinating and rapidly growing directions within the research area of nonlinear dynamics.

Generally, **controlling chaos** is regarded as processes or mechanisms that purposefully change a chaotic motion to achieve a regular motion. Specifically, controlling chaos consists of suppression, direction, and control of chaos. **Suppression of chaos** eliminates chaotic motion while applies no requirements on the resulting motion. **Direction of chaos** targets a chaotic trajectory in the state space to a small neighborhood of previously prescribed points, circles or tori. **Control of chaos** is to manipulate a chaotic motion via an actively applied input in order to track a desired regular motion. Its special but significant case is stabilization of chaos that transforms one of an infinite number of unstable periodic orbits embedded within the chaotic attractor to stable ones. Suppression of chaos is, in the broadest sense, removing chaotic motions regardless of the outcomes. Direction of chaos is usually a necessary preparation for control of chaos. Control of chaos has the strict meaning that the controlled motion should be a periodic one with a previously given amplitude and period. Only control of chaos will be covered in this chapter.

Controlling chaos is widely investigated because of its theoretical importance and possible applications. Academically, controlling chaos is a new stage of the development of chaos theory. The development begins with the focus on the transition from order to chaos, including conditions, mechanisms, and routes of chaos occurrence. Order within chaos was then revealed as universality in chaos, statistical characteristics of chaos, and fractal structures of chaos. At the present stage, the processes that form chaos to order can be implemented via the active control. Practically, controlling chaos is an essential step toward the application of chaos theory. Controlling chaos can not only remove chaotic motion from a system when chaos is harmful but also take advantage of some aspects of chaos such as the extreme sensitivity to initial states. For example, based on the sensitivity of the three-body problem to small perturbations, NASA scientists utilized small amounts of residual fuel to send the spacecraft ISEE-3/IEC more than 50 million miles across the solar system, achieving the first scientific cometary encounter. Due to control of chaos, if a system is designed for several purposes or under diverse conditions at different times, purposefully building chaos into the system may allow the desired flexibilities for multiple uses.

5.1.2 Problem Formulations

As stated above, the problem of control of chaos contains a specified chaotic system to be controlled and a regular motion as the desired control goal, construction of a control law such that the controlled system display the desired motion. In order to facilitate the study of control design later, a formal definition of the problem is presented as follows. Consider a nonlinear system governed by a set of ordinary differential equations

$$\dot{\mathbf{x}} = \mathbf{f}(\mathbf{x}, t, \mathbf{u}) \quad (5.1.1)$$

with an observable output function

$$\mathbf{y} = \mathbf{h}(\mathbf{x}, t, \mathbf{u}) \quad (5.1.2)$$

where t is the time variable, $\mathbf{x} \in R^m$ is the state variable, $\mathbf{u} \in R^n$ is the control input, and $\mathbf{y} \in R^l$ are the output variable. If no control is applied, e.g. $\mathbf{u} = \mathbf{0}$, one or more components of \mathbf{y} are chaotic. For a desired regular goal $\mathbf{y}_d(t)$, a control law

$$\mathbf{u} = \mathbf{g}(\mathbf{x}, t) \quad (5.1.3)$$

is designed for the input \mathbf{u} , such that starting from any initial state in a region, within the precision of measurement, the desired regular motion

$$\mathbf{y}(t) = \mathbf{y}_d(t) \quad (5.1.4)$$

can be realized for all $t > t_0$ (a given time instant). If the control law (5.1.3) is independent of the state \mathbf{x} , the control is called an **open-loop control**. If the control law (5.1.3) depends on both time t and state \mathbf{x} , the control is called a **closed-loop control** or **feedback control**. If the control goal $\mathbf{y}_d(t)$ is one of the unstable solutions of Eq. (5.1.1), namely,

$$\dot{\mathbf{y}}_d = \mathbf{f}(\mathbf{y}_d, t, \mathbf{u}) \quad (5.1.5)$$

then it is the problem of chaos stabilization. In the following, the output variables are simply some state variables.

As formulated above, control of chaos is actually a tracking problem [2] in which the tracking goal is a periodic motion and the system to be controlled is chaotic. Therefore, the approaches developed for control of chaos are neither exclusive of nor conflictive with the established control strategies in system theory or control engineering. In fact, chaos can be successfully controlled via various methods, such as conventional linear feedback control, feedback linearization, optimal control, stochastic control, adaptive control, and intelligent control. On the other hand, control of chaos seeks to develop new theories and methods that are particularly appropriate for chaotic motions.

There are some qualitative specifications in the design of a control law for a nonlinear system. Stability must be guaranteed for the controlled system at least for reasonably large region of initial states. Accuracy and speed of response should be examined as the control performance. Robustness should be taken into consideration. Robustness is the insensitivity to effects that are not modeled. The controlled system should be able to withstand these neglected effects. The energy needed by the control, reflected in the control input should be as small as possible. However, the above-mentioned qualities conflict to some extent, and a good control design can be proposed only based on the effective trade-offs in terms of stability/robustness, stability/performance, performance/energy-saving, and so on.

5.1.3 OGY Method and Its Generalization

The OGY method is based on the geometrical structure of chaotic attractors. The control goal must be one of the infinitely many unstable periodic orbits embedded in the chaotic attractor. The unstable periodic orbit is stabilized via the linear feedback control. To highlight the essence of the method, only the stabilization of a fixed point is addressed.

Consider a 2-dimensional map with an adjustable parameter as the control input

$$\mathbf{z}_{i+1} = \mathbf{M}(\mathbf{z}_i, u_i) \quad (\mathbf{z}_i \in R^2) \quad (5.1.6)$$

If no control is applied, e.g. $u_i=0$, map (5.1.6) has a chaotic attractor in which a unstable fixed point is located that needs to be stabilized

$$\mathbf{z}_F = \mathbf{M}(\mathbf{z}_F, 0) \quad (5.1.7)$$

Local linearization of Eq. (5.1.6) in the neighborhood of $(\mathbf{z}_F, 0)$ yields

$$\mathbf{z}_{i+1} - \mathbf{z}_F = \mathbf{D}_z \mathbf{M}(\mathbf{z}_i - \mathbf{z}_F) + \frac{\partial \mathbf{M}}{\partial u} u_i \quad (5.1.8)$$

where the 2×2 Jacobian matrix $\mathbf{D}_z \mathbf{M}$ and 2-dimensional vector $\partial \mathbf{M} / \partial u$ are both calculated at $(\mathbf{z}_F, 0)$. Assume that the eigenvalues λ_s and λ_u of $\mathbf{D}_z \mathbf{M}$ satisfy $|\lambda_s| < 1$ and $|\lambda_u| > 1$. Then the eigenvectors \mathbf{e}_s and \mathbf{e}_u corresponding to λ_s and λ_u determine the stable and unstable directions in the small neighborhood of $(\mathbf{z}_F, 0)$. Denote the contravariant eigenvectors of \mathbf{e}_s and \mathbf{e}_u as \mathbf{f}_s and \mathbf{f}_u such that

$$\mathbf{f}_s^T \cdot \mathbf{e}_s = \mathbf{f}_u^T \cdot \mathbf{e}_u = 1, \quad \mathbf{f}_s^T \cdot \mathbf{e}_u = \mathbf{f}_u^T \cdot \mathbf{e}_s = 0 \quad (5.1.9)$$

then

$$\mathbf{D}_z \mathbf{M} = \lambda_s \mathbf{e}_s \mathbf{f}_s^T + \lambda_u \mathbf{e}_u \mathbf{f}_u^T \quad (5.1.10)$$

Therefore, if the control law is designed as

$$u_i = -\frac{\lambda_u}{\mathbf{f}_u \cdot \frac{\partial \mathbf{M}}{\partial \mathbf{u}}} \mathbf{f}_u \cdot (\mathbf{z}_i - \mathbf{z}_F) \quad (5.1.11)$$

then Eqs. (5.1.8), (5.1.9), (5.1.10), and (5.1.11) lead to

$$\mathbf{f}_u \cdot (\mathbf{z}_{i+1} - \mathbf{z}_F) = 0 \quad (5.1.12)$$

Equation (5.1.12) implies that the control law (5.1.11) moves \mathbf{z}_{i+1} into the stable direction of \mathbf{z}_F . Hereafter, the control is unnecessary until \mathbf{z}_{i+1} drifts away from the stable direction. In that case, the control law should be actuated again. This original idea was proposed by Ott, Grebogi and Yorke in 1990. Hence it is called the Ott-Grebogi-Yorke method or OGY method.

The above idea can be extended to higher-dimensional maps [3]. Consider an n -dimensional map with a controllable parameter

$$\mathbf{z}_{i+1} = \mathbf{M}(\mathbf{z}_i, u_i) \quad (\mathbf{x}_n \in R^n) \quad (5.1.13)$$

If $u_i = 0$, a fixed point

$$\mathbf{z}_F = \mathbf{M}(\mathbf{z}_F, 0) \quad (5.1.14)$$

embedded in the chaotic attractor is the control goal. Local linearization of Eq. (5.1.13) in the neighborhood of $(\mathbf{z}_F, 0)$ gives

$$\mathbf{z}_{i+1} - \mathbf{z}_F = \mathbf{A}(\mathbf{z}_i - \mathbf{z}_F) + \mathbf{B}u_i \quad (5.1.15)$$

where both the $n \times n$ Jacobian matrix $\mathbf{A} = \mathbf{D}_x \mathbf{M}(\mathbf{x}, u)$ and $n \times 1$ Jacobian matrix $\mathbf{B} = \mathbf{D}_u \mathbf{M}(\mathbf{x}, u)$ are calculated at $(\mathbf{x}, u) = (\mathbf{x}_F, 0)$. To stabilize \mathbf{x}_F , let us introduce a linear feedback control law

$$u_i = \mathbf{k}^T (\mathbf{z}_i - \mathbf{z}_F) \quad (5.1.16)$$

where \mathbf{k}^T is the transpose of $n \times 1$ matrix \mathbf{k} to be determined later. Substitution of Eq. (5.1.6) into Eq. (5.1.15) leads to

$$\mathbf{z}_{i+1} - \mathbf{z}_F = (\mathbf{A} + \mathbf{B}\mathbf{k}^T)(\mathbf{z}_i - \mathbf{z}_F) \quad (5.1.17)$$

which implies that the fixed point \mathbf{x}_F is stable on the condition that all eigenvalues of the $n \times n$ matrix $\mathbf{A} + \mathbf{B}\mathbf{k}^T$ have modulus smaller than 1. The solution to the problem of the determination of \mathbf{k} for given \mathbf{A} and \mathbf{B} such that the eigenvalues of the matrix $\mathbf{A} + \mathbf{B}\mathbf{k}^T$ have specified values is well known in system theory. The eigenvalues of the matrix $\mathbf{A} + \mathbf{B}\mathbf{k}^T$ are called the regulator poles, and the problem is called the pole placement problem. There is a standard algorithm, Ackermann's

method [4]. Obviously, the choices of poles are not unique. A natural and effective choice is setting n_s of these poles equal to the eigenvalues of A with modulus smaller than 1 and the remaining $n - n_s$ poles to zero. Under this circumstance, the control law (5.1.16) makes z_{i+1} into the local stable manifold of z_F .

The method is proposed for maps, but it can also be applied to systems governed by differential equations via the Poincaré map. In the method, the control goal must be an unstable periodic orbit embedded in the chaotic attractor, and thus the method only solves the stabilization of chaos. The control energy needed is reasonably small, as the intrinsic stable directions are used. Because the method is based on the local linearization, the control law can be actuated only if the chaotic trajectory is sufficiently close to the goal. In the absence of noise, the control input can be arbitrarily small, while it needs a long time to wait for the chaotic trajectory to enter a very small neighborhood of the goal. To increase the effectiveness of the method, direction of chaos can be performed to target the chaotic trajectory to the desired neighborhood of the goal.

5.1.4 Synchronization: Chaos Control in a Broader Sense

In a broader sense, chaos control is a process or a mechanism that suppresses existing chaotic motion when it is harmful, as well as creates chaotic motion or enhances chaotic motion when it is beneficial or useful. Making an original regular motion chaotic is referred as **anticontrol of chaos** or **chaotification**. Therefore, chaos control concerns two systems, which may be identical, one to be controlled and the other to be achieved. In this view, chaos control may be regarded as a special case of system synchronization.

Synchronization literally means correlated time-dependent behavior between different processes that interact with each other in one way or another. The relevant research on synchronization can be dated back to Huygens who investigated frequency locking between two clocks, which is perhaps first nonlinear phenomenon observed. Synchronization has become an active research topic in nonlinear dynamics since the early 1990s when researchers realized that chaotic systems can be synchronized and recognized its potential for communications [5]. A unifying definition of synchronization is proposed for systems with control inputs as follows [6].

Consider two finite dimensional systems governed by the ordinary differential equations

$$\dot{x}_i = f_i(x_1, x_2, t, u) \quad (i = 1, 2) \quad (5.1.18)$$

with the observable output functions

$$y_i = h_i(x_1, x_2, t, u) \quad (i = 1, 2) \quad (5.1.19)$$

where t is the time variable, $\mathbf{x}_i \in R^{m_i}$ is the state variables, $\mathbf{u} \in R^n$ is the control input, and $\mathbf{y}_i \in R^l$ are the output variables. If there exists the control law

$$\mathbf{u} = \mathbf{g}(\mathbf{x}_1, \mathbf{x}_2, t) \quad (5.1.20)$$

such that, within the measuring precision,

$$\mathbf{y}_1(t) = \mathbf{y}_2(t) \quad (5.1.21)$$

for all $t > t_0$ (a given time instant), there is **synchronization** at beginning time t_0 between the two systems (5.1.18) with respect to the output functions (5.1.19).

In the above-mentioned definition, no details of initial conditions are involved. Actually, initial conditions are crucial in nonlinear systems, especially chaotic systems. Synchronization with respect to initial conditions can be divided into two classes. Local synchronization holds only for trajectories starting in small neighborhoods of given initial states, while global synchronization holds for all trajectories. In fact, there is a special synchronization problem to identify chaotic behaviors of a dynamical system for different initial conditions, which may be regarded as the two dynamical systems defined here being identical.

According to the definition presented here, both widely studied control of chaos and newly proposed anticontrol of chaos are essentially synchronization of dynamical systems. In fact, controlling chaos is the synchronization between a specific chaotic system to be controlled and a prescribed periodical system. The anti-control of chaos is the synchronization between a specific non-chaotic system and a chaotic system, usually not prescribed.

5.2 The Parametric Open-plus-closed-loop Method

5.2.1 Introduction

In 1990, Jackson advanced the **entrainment control** [7], which is the development of the **resonant control** [8] presented by Hübler and Lüscher in 1989, one of the earliest methods of controlling chaos. Its essence is to design an external excitation based on the control goal, as the open-loop control, so that the control goal is a particular solution of the controlled system. To ensure the stability of a particular solution, it is required that the control goal be in suitable regions of the state space (called **convergent regions**) and there be suitable initial conditions (called the **basin of entrainment**) when the control is activated [9, 10]. The entrainment control established by Jackson is suitable for the systems with additive controllable parameters. Extension of its idea to the systems without additive controllable parameters forms the **parametric entrainment control** [11]. Both the entrainment control and the parametric entrainment control have two

restrictions. The system must be dissipative, because the convergent region exists only in this case. The unstable periodic orbits of the uncontrolled system cannot be the goal of the control, that is, the methods cannot be applied to solve the problems of stabilization. In addition, the convergent regions and the basin of entrainment are difficult to determine in practical applications.

In 1995, Jackson and Grosu advanced an **open-plus-closed-loop control** based on the entrainment control [12]. For systems with additive controllable parameters, introducing a closed-loop part into the entrainment control law remedies its defects, and may be implemented in experiments [13]. In fact, the basin of entrainment in the open-plus-closed-loop control for all classic chaotic systems is infinitely large [12]. The authors modified the approach to control nonlinear oscillators governed by non-autonomous second-order ordinary differential equations [14]. For systems without additive controllable parameters, the authors developed a **parametric open-plus-closed-loop control** [15], which will be presented in this section. The necessary inputs of the control and the robustness of the control will be discussed in numerical examples. The final subsection will clarify the relations among the entrainment control, the parametric entrainment control, the open-plus-close-loop control, and the parametric open-plus-closed-loop control, as well as the differences between the controls of an oscillator and a general dynamical system.

5.2.2 The Control Law

Consider a controllable inertial uncoupling nonlinear oscillation system with n degrees-of-freedom

$$\ddot{\mathbf{q}} = \mathbf{f}(\mathbf{q}, \dot{\mathbf{q}}, \mathbf{u}, t) \quad (5.2.1)$$

where n dimensional vectors \mathbf{q} , $\dot{\mathbf{q}}$ and $\ddot{\mathbf{q}}$ are the generalized coordinate, velocity and acceleration, respectively, n dimensional vector \mathbf{u} is a control parameter, and t is the time variable. Assume that the system displays chaotic motion when no control is applied ($\mathbf{u} = \mathbf{0}$). Give a periodic control goal $\mathbf{q}_g(t)$. The local linearization of Eq. (5.2.1) in the neighborhood of $(\mathbf{q}_g, \dot{\mathbf{q}}_g, t, \mathbf{0})$ leads to

$$\ddot{\mathbf{q}} = \mathbf{f}(\mathbf{q}_g, \dot{\mathbf{q}}_g, t, \mathbf{0}) + \mathbf{D}_{\dot{\mathbf{q}}} \mathbf{f}(\dot{\mathbf{q}} - \dot{\mathbf{q}}_g) + \mathbf{D}_{\mathbf{q}} \mathbf{f}(\mathbf{q} - \mathbf{q}_g) + \mathbf{D}_{\mathbf{u}} \mathbf{f} \cdot \mathbf{u} \quad (5.2.2)$$

where the Jacobians

$$\mathbf{D}_{\mathbf{u}} \mathbf{f} = \left[\frac{\partial f_i}{\partial u_j} \right]_{n \times n}, \quad \mathbf{D}_{\dot{\mathbf{q}}} \mathbf{f} = \left[\frac{\partial f_i}{\partial \dot{q}_j} \right]_{n \times n}, \quad \mathbf{D}_{\mathbf{q}} \mathbf{f} = \left[\frac{\partial f_i}{\partial q_j} \right]_{n \times n} \quad (5.2.3)$$

are evaluated at $(\mathbf{q}_g, \dot{\mathbf{q}}_g, t, \mathbf{0})$. Assume $\mathbf{D}_{\mathbf{u}} \mathbf{f}$ be an inevitable matrix. Let

$$\mathbf{u} = (\mathbf{D}_u \mathbf{f})^{-1} \left[\ddot{\mathbf{q}}_g - \mathbf{f}(\mathbf{q}_g, \dot{\mathbf{q}}_g, t, \mathbf{0}) + (\mathbf{D}_q \mathbf{f} - \mathbf{A})(\dot{\mathbf{q}}_g - \dot{\mathbf{q}}) + (\mathbf{D}_q \mathbf{f} - \mathbf{B})(\mathbf{q}_g - \mathbf{q}) \right] \quad (5.2.4)$$

where the $n \times n$ matrices of both \mathbf{A} and \mathbf{B} are diagonal

$$\mathbf{A} = \text{diag}[\alpha_1, \alpha_2, \dots, \alpha_n], \quad \mathbf{B} = \text{diag}[\beta_1, \beta_2, \dots, \beta_n] \quad (5.2.5)$$

with the undetermined elements α_i and β_j ($i, j = 1, 2, \dots, n$). Substitution of Eq. (5.2.4) into Eq. (5.2.5) yields

$$(\ddot{\mathbf{q}} - \ddot{\mathbf{q}}_g) + \mathbf{A}(\dot{\mathbf{q}} - \dot{\mathbf{q}}_g) + \mathbf{B}(\mathbf{q} - \mathbf{q}_g) = 0 \quad (5.2.6)$$

Hence coefficients α_i and β_j ($i, j = 1, 2, \dots, n$) can be determined by a normal design principle, such as pole placement, linear-quadratic optimal regulator, or robust service regulator, so that the differential equations

$$\ddot{y}_i + \alpha_i \dot{y}_i + \beta_i y_i = 0 \quad (i = 1, 2, \dots, n) \quad (5.2.7)$$

have asymptotically stable zero solutions.

Notice that the control input determined by Eq. (5.2.4) is composed of two parts. The open-loop part without feedback is

$$\mathbf{u}_o = (\mathbf{D}_u \mathbf{f})^{-1} \left[\ddot{\mathbf{q}}_g - \mathbf{f}(\mathbf{q}_g, \dot{\mathbf{q}}_g, t, \mathbf{0}) \right] \quad (5.2.8)$$

and the closed-loop part with feedback is

$$\mathbf{u}_c = (\mathbf{D}_u \mathbf{f})^{-1} \left[(\mathbf{D}_q \mathbf{f} - \mathbf{A})(\dot{\mathbf{q}}_g - \dot{\mathbf{q}}) + (\mathbf{D}_q \mathbf{f} - \mathbf{B})(\mathbf{q}_g - \mathbf{q}) \right] \quad (5.2.9)$$

Besides, the system in (5.2.1) is not required to have additive controllable parameters. Therefore Eq. (5.2.4) gives a **parametric open-plus-closed-loop control law**.

Suppose to start control when $t = t_1$. To make Eq. (5.2.1) approximate Eq. (5.2.2) sufficiently well, the control should be actuated in a small neighborhood of $(\mathbf{q}_g, \dot{\mathbf{q}}_g, t, \mathbf{0})$. Hence the parametric open-plus-closed-loop control law takes the form

$$\begin{aligned} \mathbf{u} = & (\mathbf{D}_u \mathbf{f})^{-1} S(t - t_1) S(\varepsilon - |\mathbf{q}_g - \mathbf{q}| - |\dot{\mathbf{q}}_g - \dot{\mathbf{q}}|) \left[\ddot{\mathbf{q}}_g - \mathbf{f}(\mathbf{q}_g, \dot{\mathbf{q}}_g, t, \mathbf{0}) \right. \\ & \left. + (\mathbf{D}_q \mathbf{f} - \mathbf{A})(\dot{\mathbf{q}}_g - \dot{\mathbf{q}}) + (\mathbf{D}_q \mathbf{f} - \mathbf{B})(\mathbf{q}_g - \mathbf{q}) \right] \end{aligned} \quad (5.2.10)$$

where ε is a small positive real number, and the switch function is defined by

$$S(z) = \begin{cases} 0 & z \leq 0 \\ 1 & z > 0 \end{cases} \quad (5.2.11)$$

In this chapter, only the nonlinear oscillator with one degree-of-freedom will

be treated. For such an oscillator

$$\ddot{q} = f(q, \dot{q}, u, t) \quad (5.2.12)$$

where q , \dot{q} and \ddot{q} are the generalized coordinate, generalized velocity and generalized acceleration, respectively, u is a control parameter, and t is the time variable. For a given control goal q_g , the parametric open-plus-closed-loop control law starting at $t = t_1$ is designed as

$$u = \frac{1}{f'_u} S(t - t_1) S(\varepsilon - |q_g - q| - |\dot{q}_g - \dot{q}|) \left[\ddot{q}_g - f(q_g, \dot{q}_g, 0, t) + (f'_q + \alpha)(\dot{q}_g - \dot{q}) + (f'_q + \beta)(q_g - q) \right] \quad (5.2.13)$$

where α and β can be determined via placing the poles of equation

$$(\ddot{q} - \ddot{q}_g) + \alpha(\dot{q} - \dot{q}_g) + \beta(q - q_g) = 0 \quad (5.2.14)$$

such that the solution asymptotically tends to zero.

5.2.3 Numerical Examples

The forced Duffing oscillator with a controllable parameter

$$\ddot{q} = -0.2\dot{q} + (1 + u)q - q^3 + 0.3 \cos t \quad (5.2.15)$$

is treated as an example to demonstrate the application of the parametric open-plus-closed-loop control. Chaotic behavior appears without control. The control goals successively are an equilibrium point and a period 2 motion

$$q_g(t) = 1 \quad (5.2.16)$$

$$q_g(t) = 0.5 + 0.4 \sin 0.5t \quad (5.2.17)$$

The control goals (5.2.16) and (5.2.17) satisfy $f'_u \neq 0$ evaluated at $(q_g, \dot{q}_g, 0, t)$. Let $\varepsilon = 1.0$, and the control is started after $t_1 = 40.0$.

The coefficients α and β are determined by the pole assignment. The roots of the characteristic polynomial associated with the closed-loop system

$$r^2 + \alpha r + \beta = 0 \quad (5.2.18)$$

should have negative real parts. Hence choose $\alpha = 2.8$ and $\beta = 4.0$.

The control can be implemented via the classical nonlinear system approaches, such as input-output linearization. The results for two goals are shown in Figs. 5.1 and 5.2, respectively. The solid lines denote the time histories of the system subjected

to the parametric open-plus-closed-loop control law (5.2.13). The dashed lines denote the time histories of the system subjected to the input-output linearization control law. The dot lines denote the time histories of the uncontrolled system. In this example, the parametric open-plus-closed-loop control has a slightly longer time transition to achieve the goals than that of the input-output linearization control.

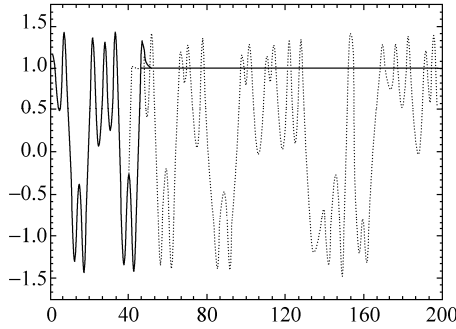


Figure 5.1 Controlling chaos to the equilibrium point

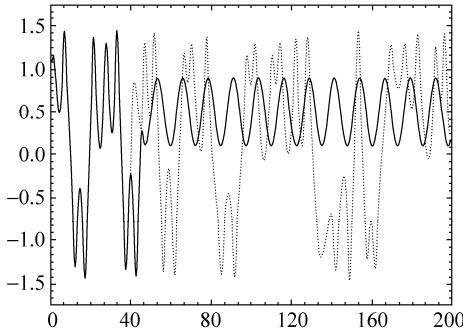


Figure 5.2 Controlling chaos to the period motion

The control inputs $u = u(t)$ for two goals are shown in Figs. 5.3 and 5.4, respectively. The solid lines denote the control signals given by Eq. (5.2.13), and the dashed lines denote the control signals given by the input-output linearization control. For both goals, a great pulse input is needed to activate the input-output linearization control. Since the parametric open-plus-closed-loop control starts just when the chaotic phase trajectory is closed to the goal periodic orbit, only a small pulse input is needed. Directly applying the input-output linearization control in the neighborhood of the goal gives the same results, but the nonlinear control law is not necessary in this case. In most practical circumstances, linear control laws are easy to implement.

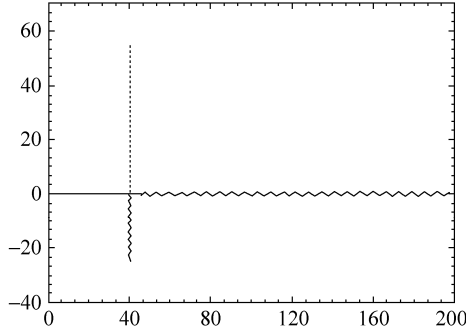


Figure 5.3 Control inputs for the equilibrium point

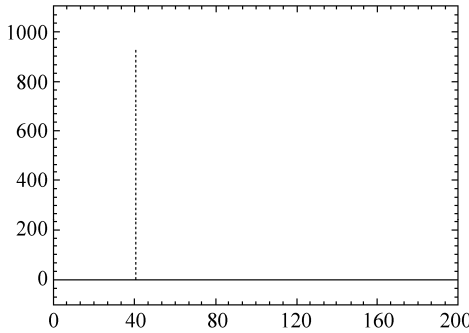


Figure 5.4 Control inputs for the period motion

The following example focuses on the robustness. Although the parametric open-plus-closed-loop control law (5.2.13) is model-based, the following example indicates that it is robust to model errors. Let us consider the forced oscillator with an additive controllable parameter

$$\ddot{q} = -0.2\dot{q} + q - 0.05q^2 - q^3 + 0.3 \cos \omega t + u \tag{5.2.19}$$

Chaos occurs in it if $u=0$. The control goals successively are an equilibrium point and a period 2 motion

$$q_g(t) = 0 \tag{5.2.20}$$

$$q_g(t) = \sin 0.5t \tag{5.2.21}$$

Suppose that the real model governed by Eq. (5.2.19) is unknown, and the control law is designed based on the approximate model

$$\ddot{q} = -0.2\dot{q} + 1.1q - q^3 + 0.3 \cos \omega t + u \tag{5.2.22}$$

There exist both a structural error (no q^2 term) and a parametric error. Let $\varepsilon = 1.0$.

Choose $\alpha = 2.8$ and $\beta = 4.0$. Start control after $t_1 = 40.0$.

The results for both goals are shown in Figs. 5.5 and 5.6, respectively. The solid lines denote the time histories of the controlled system, and the dot lines denote the time histories of the uncontrolled system. The control error is defined as the difference between the system output and the desired goal. As shown in Figs. 5.7

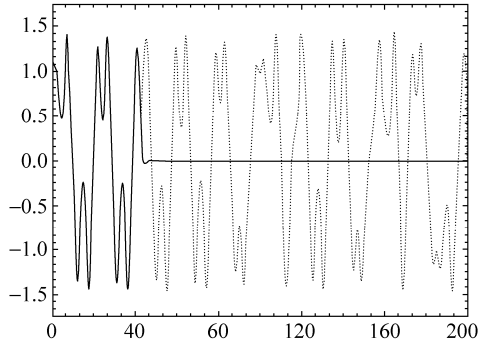


Figure 5.5 Control of chaos to the equilibrium point

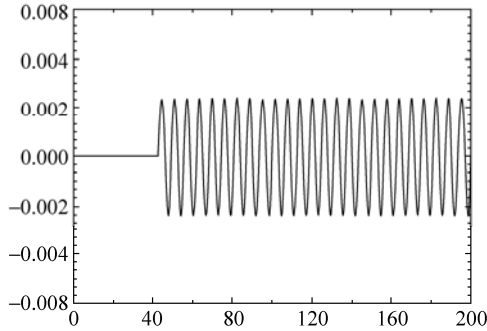


Figure 5.6 Control error to the equilibrium point

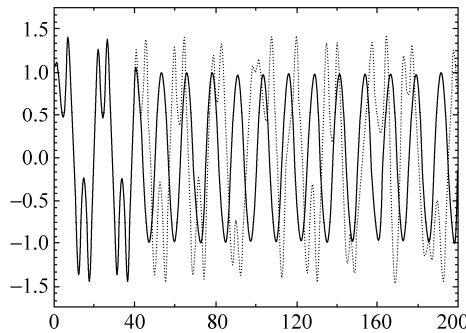


Figure 5.7 Control of chaos to the periodic motion

and 5.8, the control errors are small. Therefore the real system governed by Eq. (5.2.19) may be controlled sufficiently well by the control law (5.2.13) designed based on the model system represented by Eq. (5.2.20) if the model error is small enough.

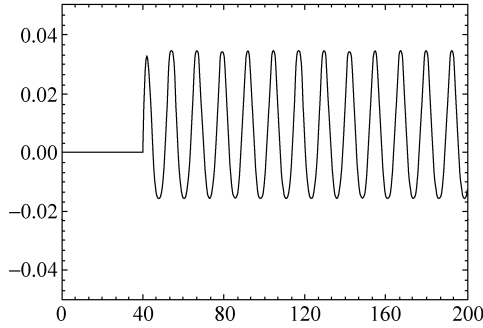


Figure 5.8 Control error to the periodic motion

5.2.4 Discussions

The parametric open-plus-closed-loop control law can also be proposed for a general dynamical system (5.1.1) as

$$\mathbf{u} = (\mathbf{D}_u \mathbf{f})^{-1} [\mathbf{x}_g - \mathbf{f}(\mathbf{x}, t, \mathbf{0}) + (\mathbf{D}_x \mathbf{f} - \mathbf{B}(t))(\mathbf{x}_g - \mathbf{x})] \quad (5.2.23)$$

where \mathbf{x}_g is the control goal and the matrix function $\mathbf{B}(t)$ provides the solution to

$$\dot{\mathbf{y}} + \mathbf{B}(t)\mathbf{y} = \mathbf{0} \quad (5.2.24)$$

asymptotically tending to zero. In practical designs, $\mathbf{B}(t)$ can be chosen as a constant matrix whose all eigenvalues have negative real parts.

For a system with an additive control input

$$\dot{\mathbf{x}} = \mathbf{f}(\mathbf{x}, t) + \mathbf{u} \quad (5.2.25)$$

$\mathbf{D}_u \mathbf{f}$ is the unit matrix. Thus Eq. (5.2.23) leads to the open-closed-loop control law. If one lets

$$\mathbf{B}(t) = \mathbf{D}_x \mathbf{f} \quad (5.2.26)$$

then Eqs. (5.2.23) and (5.2.25) yield respectively the parametric entrainment control law and the entrainment control law.

The control law (5.2.23) can be employed to control nonlinear oscillators governed by non-autonomous second-order ordinary differential equations. Nevertheless

the number of control inputs required by the open-plus-closed-loop control for general dynamical systems defined by Eq. (5.2.25) is equal to the dimension of state spaces. Consider a nonlinear oscillator with one degree-of-freedom, 2 control inputs are needed. The controlled system should take the form

$$\begin{aligned}\dot{x}_1 &= x_2 + v(x_1, x_2, t) \\ \dot{x}_2 &= f(x_1, x_2, t) + u(x_1, x_2, t)\end{aligned}\tag{5.2.27}$$

where x_1 and x_2 are state variables, and u and v are controllable inputs. In some practical circumstances, there may be no such controllable inputs available. Section 5.2.2 developed a control approach that requires only one control parameter. The controlled system should take the form

$$\begin{aligned}\dot{x}_1 &= x_2 \\ \dot{x}_2 &= f(x_1, x_2, t) + u(x_1, x_2, t)\end{aligned}\tag{5.2.28}$$

or more general

$$\begin{aligned}\dot{x}_1 &= x_2 \\ \dot{x}_2 &= f(x_1, x_2, u(x_1, x_2, t), t)\end{aligned}\tag{5.2.29}$$

5.3 The Stability Criterion Method

5.3.1 Introduction

This section presents a method for controlling chaos in the form of special nonlinear feedback proposed by Yu, Liu and Peng [16]. The method is inspired by Pyragas's continuous linear feedback control method [17] and Ushio's contraction mapping control method of discrete systems [18]. The validity of the method is based on the stability criterion of linear system, and it can be called **the stability criterion method**. The construction of a special form of a time-continuous perturbation feedback in the stability criterion method does not change the form of the desired unstable periodic orbit. The close return pairs technique [19] is utilized to estimate a desired periodic orbit chosen from numerous unstable periodic orbits embedded within a chaotic attractor. This method does not require linearization of the system around the stabilized orbit and calculation of the derivative at unstable periodic orbits. As examples of numerical simulations, the control of the Rössler system and the control of two coupled Duffing oscillators are investigated. The complexity of the experimental realization of the stability criterion method is mainly to input the desired unstable periodic orbits. Besides, the

method relies on the explicit knowledge of the mathematical model of the system.

In this section, the stability criterion method is proposed only for the stabilization problem, while the idea can be employed to solve the tracking problem. The idea was also implemented in the synchronization of chaos [20].

5.3.2 The Control Law

Consider a system with an additive control input defined by Eq. (5.2.25). The system without control ($\mathbf{u} = \mathbf{0}$) has a chaotic attractor. Decompose the vector function $\mathbf{f}(\mathbf{x}, t)$ into a suitably chosen linear part and the other nonlinear part

$$\mathbf{f}(\mathbf{x}, t) = \mathbf{A}\mathbf{x} + \mathbf{h}(\mathbf{x}, t) \quad (5.3.1)$$

where \mathbf{A} is a constant matrix whose all eigenvalues have negative real parts and $\mathbf{h}(\mathbf{x}, t)$ is a nonlinear function. Let the control goal $\mathbf{x}_g(t)$ be an unstable periodic orbit embedded within the chaotic attractor. Then

$$\dot{\mathbf{x}}_g = \mathbf{A}\mathbf{x}_g + \mathbf{h}(\mathbf{x}_g, t) \quad (5.3.2)$$

Design the control input as

$$\mathbf{u} = \mathbf{h}(\mathbf{x}_g, t) - \mathbf{h}(\mathbf{x}, t) \quad (5.3.3)$$

Substitution of Eq. (5.3.1) into Eq. (5.3.3) leads to the nonlinear feedback control law

$$\mathbf{u} = \mathbf{A}(\mathbf{x} - \mathbf{x}_g) + \mathbf{f}(\mathbf{x}_g, t) - \mathbf{f}(\mathbf{x}, t) \quad (5.3.4)$$

Equations (5.2.25), (5.3.1), (5.3.2) and (5.3.3) yield the governing equation of the controlled system

$$\dot{\mathbf{x}} - \dot{\mathbf{x}}_g = \mathbf{A}(\mathbf{x} - \mathbf{x}_g) \quad (5.3.5)$$

Because all eigenvalues of matrix \mathbf{A} have negative real parts, the stability criterion of linear systems guarantees the zero solution of the following equation

$$\dot{\mathbf{y}} = \mathbf{A}\mathbf{y} \quad (5.3.6)$$

is asymptotically stable. Therefore the controlled trajectory $\mathbf{x}(t)$ tends asymptotically to the goal $\mathbf{x}_g(t)$. It implies that the unstable periodic orbit is stabilized. Note that the control input $\mathbf{u}(t)$ becomes zero after the state when the controlled system converges to the unstable periodic orbits.

Some very complicated periodically driven dynamical systems along with the stabilized unstable periodic orbit can have alternative stable solutions belonging

to different basins of initial conditions. Besides, large initial values of the control input can be also undesired for some experiments. Such problems can be solved by restriction of the control input. Therefore the stabilization is achieved by small input values if Eq. (5.3.4) is modified as follows

$$\mathbf{u} = \begin{cases} \mathbf{A}(\mathbf{x} - \mathbf{x}_g) + \mathbf{f}(\mathbf{x}_g, t) - \mathbf{f}(\mathbf{x}, t) & \text{if } |\mathbf{x} - \mathbf{x}_g| < \varepsilon \\ \mathbf{0} & \text{otherwise} \end{cases}$$

where $\varepsilon > 0$ is a restriction value of error within which $\mathbf{u} \neq \mathbf{0}$. The control input has a simple form as shown in Eq. (5.3.7). It is unnecessary to calculate any derivatives at the unstable periodic orbit of the uncontrolled system, while some Jacobian matrixes are required in the open-plus-closed-loop control.

In order to obtain the necessary information on an appropriate location of a desired periodic orbit $\mathbf{x}_g(t)$, the strategy of the close return pairs described in [21, 22] is utilized. A time series of the chaotic trajectory generated by the system (5.2.25) is stroboscopically sampled in every period T when $\mathbf{u} = \mathbf{0}$. The data sampling can be used to detect the close return pairs, which consist of two successive points near each other, and indicate the existence of a periodic orbit nearby. Because of the ergodic character of orbits on a chaotic attractor, many such pairs can be obtained if the data string is long enough. Suppose that \mathbf{x}_i^1 and \mathbf{x}_i^2 are used to denote the first point and its successive point of the i -th collected return pair, $i = 1, 2, \dots, M$, respectively, where M is the maximum number of collected return pairs. When the first close return pair has been detected within a predesignated region, let us take the first point \mathbf{x}_1^1 of this pair as a reference point. Then a number of close return pairs near the reference point is

$$|\mathbf{x}_i^1 - \mathbf{x}_1^1| \leq \varepsilon_1, |\mathbf{x}_i^2 - \mathbf{x}_1^2| \leq \varepsilon_2 \quad (i = 1, 2, \dots, M) \quad (5.3.7)$$

The mean value

$$\mathbf{x}_g = \frac{1}{2M} \sum_{i=1}^M (\mathbf{x}_i^1 + \mathbf{x}_i^2) \quad (5.3.8)$$

can be regarded as an approximate fixed point. This fixed point can be used to define a restriction condition in Eq. (5.3.5).

5.3.3 Numerical Examples

The first numerical example is the Rössler system with control inputs as

$$\dot{x}_1 = -x_2 - x_3 + u_1, \dot{x}_2 = x_1 + 0.2x_2 + u_2, \dot{x}_3 = 0.2x_3(x_1 - 5.7) + u_3 \quad (5.3.9)$$

The nonlinear vector function

$$f(x, t) = \begin{pmatrix} -x_2 - x_3 \\ x_1 + 0.2x_2 \\ 0.2x_3(x_1 - 5.7) \end{pmatrix} \tag{5.3.10}$$

can be cast into Eq. (5.3.1) with

$$A = \begin{pmatrix} 0 & -1 & -1 \\ 1 & -\beta & 0 \\ 0 & 0 & -5.7 \end{pmatrix}, \quad h(x, t) = \begin{pmatrix} 0 \\ (\beta + 0.2)x_2 \\ 0.2x_1x_3 \end{pmatrix} \tag{5.3.11}$$

where β is a constant that will be determined to satisfy the stability criterion of the linear system. The eigenvalues of matrix A are

$$r_1 = -5.7, \quad r_{2,3} = -0.5(\beta \mp \sqrt{\beta^2 - 4}) \tag{5.3.12}$$

Thus all eigenvalues of matrix A have negative real parts if and only if $\beta > 0$. Equation (5.3.7) yields the following control input to stabilize the goal $x_g(t)$

$$u = \begin{cases} \begin{pmatrix} 0 \\ -(\beta + 0.2)(x_2 - x_{g2}) \\ -x_1x_3 + x_{g1}x_{g3} \end{pmatrix} & \text{if } |x - x_g| < \varepsilon \\ \mathbf{0} & \text{otherwise} \end{cases} \tag{5.3.13}$$

where $\beta > 0$.

The results of the stabilization of a period-3 motion of the Rössler system are illustrated in Figs. 5.9, 5.10, and 5.11 for $\beta = 1$, $\varepsilon = 2$, and $T = 17.5$. The constant β cannot be very large. For example, if $\beta > 11.1$, an unsuccessful control process results from the large control input u_2 . The problem can be solved by restriction of control inputs. Fix a saturating value $U_0 > 0$ for the control input, and let $u_2 = U_0$ if $u_2 \geq U_0$ and $u_2 = -U_0$ if $u_2 \leq -U_0$. Figures 5.12 and 5.13 show the results of stabilization of period-3 unstable periodic orbit within the Rössler attractor at

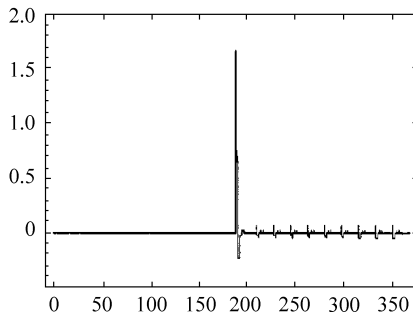


Figure 5.9 Control input u_2 to stabilize a period-3 motion

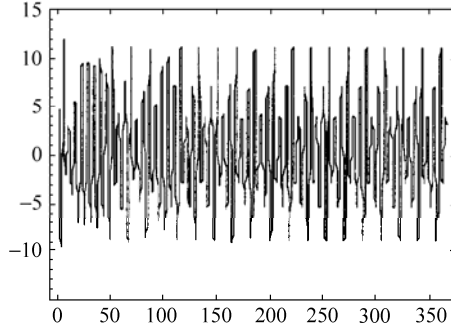


Figure 5.10 Time history of controlled state variable x_1

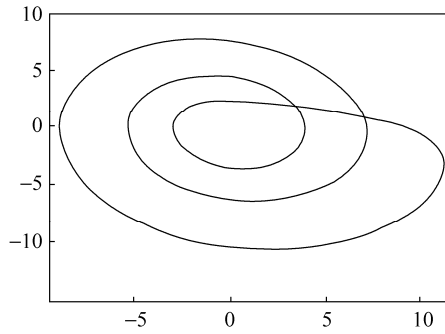


Figure 5.11 (x_1, x_3) phase portrait of the period-3 motion

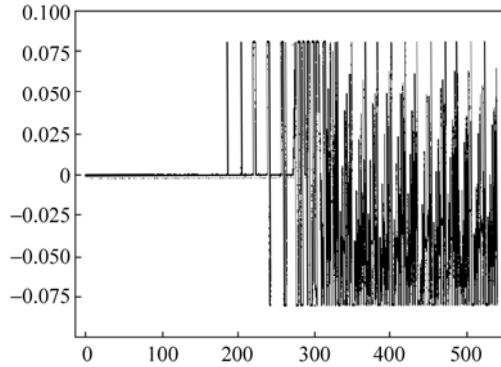


Figure 5.12 Control input with the restriction

$\beta = 13$, $\varepsilon = 2$, and $U_0 = 0.08$.

Next numerical example is a 4-dimensional nonautonomous system consisting of two coupled Duffing oscillators

$$\ddot{q}_1 + a\dot{q}_1 + q_1^3 = q_2 + b \cos t, \quad \ddot{q}_2 + c\dot{q}_2 + q_2^3 = q_1 \quad (5.3.14)$$

The first oscillator is driven by an external periodic force, and two oscillators interact

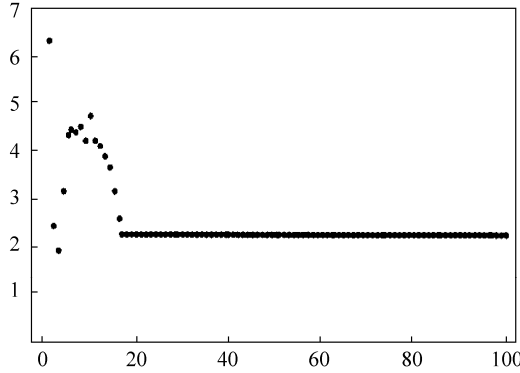


Figure 5.13 Process of stabilization of a period-3 motion: component x_1

with each other by q_1 and q_2 . When the parameters are fixed at $a = 0.2$, $b = 10.0$, and $c = 0.45$, the chaotic behavior occurs in the system. Equation (5.3.14) can be rewritten in the form of Eq. (5.2.25) after introducing the additive control inputs and letting

$$q_1 = x_1, \dot{q}_1 = x_2, q_2 = x_3, \dot{q}_2 = x_4 \tag{5.3.15}$$

Then the right hand nonlinear vector function is

$$\mathbf{f}(\mathbf{x}, t) = \begin{pmatrix} x_2 \\ -ax_2 - x_1^3 + x_3 + b \cos t \\ x_4 \\ x_1 - cx_4 - x_3^3 \end{pmatrix} \tag{5.3.16}$$

The vector function $\mathbf{f}(\mathbf{x}, t)$ can be decomposed into Eq. (5.3.1) where

$$\mathbf{A} = \begin{pmatrix} -1 & 1 & 0 & 0 \\ 0 & -a & 1 & 0 \\ 0 & 0 & -1 & 1 \\ 0 & 0 & 0 & -c \end{pmatrix}, \mathbf{h}(\mathbf{x}, t) = \begin{pmatrix} x_1 \\ -x_1^3 + b \cos t \\ x_4 \\ x_1 - x_3^3 \end{pmatrix} \tag{5.3.17}$$

the matrix \mathbf{A} has negative real eigenvalues -1 , $-a$, -1 , and $-c$. Hence it satisfies the stability condition of linear systems. Equation (5.3.7) yields the following control input to stabilize the goal $\mathbf{x}_g(t)$

$$\mathbf{u} = \begin{cases} \begin{pmatrix} -x_1 + x_{g1} \\ x_1^3 - x_{g1}^3 \\ -x_4 + x_{g4} \\ -x_1 + x_3^3 + x_{g1} - x_{g3}^3 \end{pmatrix} & \text{if } \|\mathbf{x} - \mathbf{x}_g\| < \varepsilon \\ \mathbf{0} & \text{otherwise} \end{cases} \tag{5.3.18}$$

Figures 5.14-5.16 show a chaotic trajectory in 2-dimensional subspaces (x_1, x_2) , (x_3, x_4) , and (x_1, x_3) respectively. The results of stabilization of the unstable period-1 orbit embedded in the chaotic attractor are shown in Figs. 5.17-5.19 in 2-dimensional subspaces (x_1, x_2) , (x_3, x_4) , and (x_1, x_3) .

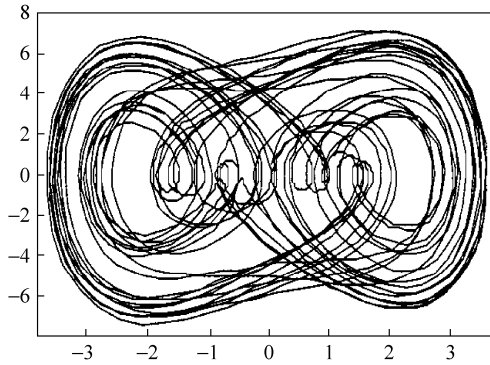


Figure 5.14 Uncontrolled chaos: subspaces (x_1, x_2)

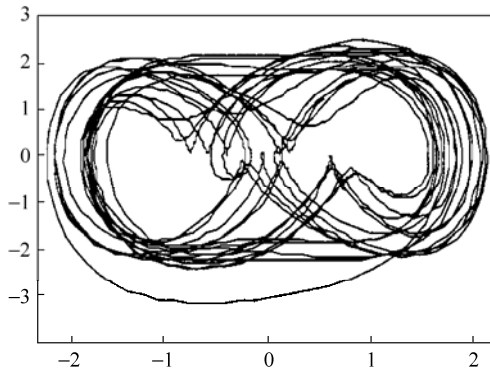


Figure 5.15 Uncontrolled chaos: subspaces (x_3, x_4)

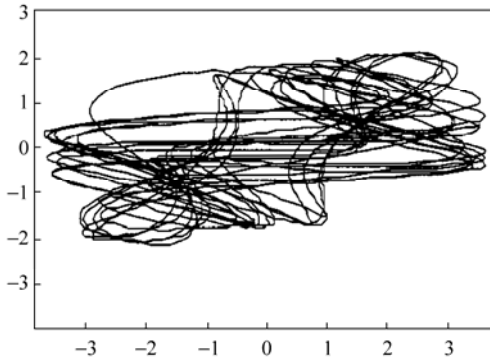


Figure 5.16 Uncontrolled chaos: subspaces (x_1, x_3)

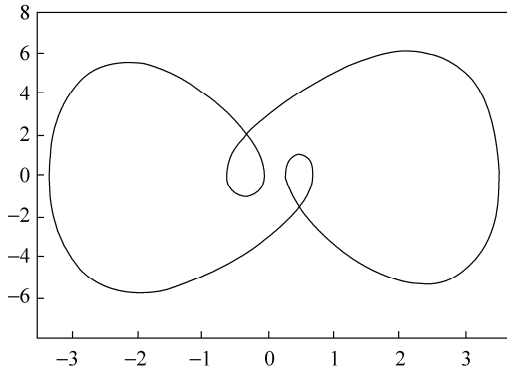


Figure 5.17 Stabilization of the period-1 motion: subspaces (x_1, x_2)

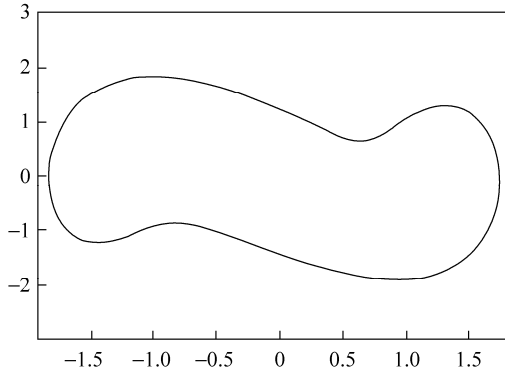


Figure 5.18 Stabilization of the period-1 motion: subspaces (x_3, x_4)

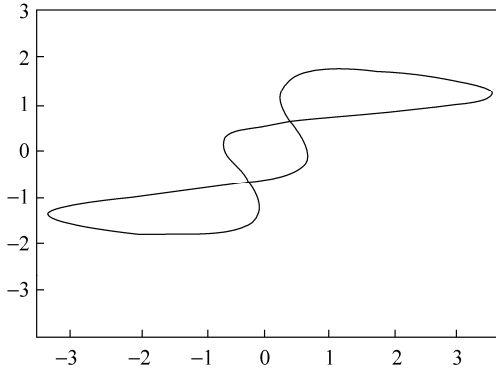


Figure 5.19 Stabilization of the period-1 motion: subspaces (x_1, x_3)

5.4 Controlling Chaotic Attitude Motions

5.4.1 Introduction

As many different control techniques are developed or employed for chaotic systems, control of chaotic attitude motion emerges as a new research direction of spacecraft attitude dynamics. Several investigators worked on the topic, and their contributions will be summarized as follows.

Dracopoulos and Jones used neural networks for modeling and genetic algorithms for control to develop a hybrid method of adaptive control [23, 24], and applied the method to control chaotic attitude motion of a rigid body spacecraft [25]. Ge, Lee, Chen, and Lee applied the continuous delayed feedback control [50] and an adaptive control [51] to regularize chaotic attitude motion of a damped satellite with partially-filled liquid [49]. Meehan and Asokanthan employed a recursive proportional feedback method [27], which is a variety of the OGY method [1], and the continuous delayed feedback method [17] to control chaotic attitude motion of a spinning spacecraft with a circumferential nutational damper [28]. Iñarraea, Lanchares, and Salas used a spinning rotor about one of the principal axes of inertia to stabilize chaotic attitude motion of a dual-spin spacecraft with time dependent moments of inertia [29]. Chen and Liu developed a parametric open-plus-closed-loop approach to control chaotic planar libration of a rigid body spacecraft in an elliptic orbit in the gravitational field with air drag and internal damping [30]. Chen and Liu revisited the problem in [31] via a modified inversion system control [30] and the input-output feedback linearization [32]. Fujii, Ichiki, Suda, and Watanabe applied the continuous delayed feedback method [17] to control chaotic planar libration of a rigid body spacecraft in an elliptic orbit in the gravitational field [33]. Tsui and Jones examined three techniques, the continuous delayed feedback method [17], a parametric control method using an artificial neural network [34], and a higher dimensional variation of the OGY method [35] in a six-dimensional system describing a rigid body spacecraft subjected to external perturbations, and found that the delayed feedback method yields the most satisfactory solution to control chaos [36]. Bernhard and Hans proposed a strategy for the deployment of a tethered satellite in a circular orbit by gravity gradient and used the chaos to fasten the process to the desired stable radial relative equilibrium [37]. Meehan and Asokanthan applied a recursive proportional feedback method [27] and the continuous delayed feedback method [17] to control chaotic attitude motion of a dual-spin spacecraft with a nutational damper [38]. They revisited the problem in [38] via a conventional energy method by minimizing the kinetic energy components associated with nutational motion that occurs during chaotic instability [39]. They also applied Lyapunov's direct method to design globally stable nonlinear control law for chaotic attitude motion of a spinning spacecraft with dissipation [40]. Chen and Liu modified the

exact feedback linearization method [41] to control chaotic attitude motion of a magnetic rigid spacecraft in a circular orbit [47] and in an elliptic orbit [48] in the gravitational and magnetic fields. Kojima, Iwasaki, Fujii, Blanksby and Trivailo proposed a decoupling and model tracking control method, combined with the delayed feedback control method, for chaotic librational motion of the tethered satellite in an elliptic orbit, with the periodic motion of a tethered satellite in a circular orbit as the reference trajectory for tracking [42]. Liu and his coworkers applied stability criterion method to control chaotic attitude motion of magnetic rigid spacecraft in a circular orbit [43, 44]. Barkow, Steindl and Troger utilized chaotic dynamics of a tethered satellite system to steer the subsatellite with small control inputs into the final radial relative equilibrium position far away from the spaceship [45]. Kuang, Meehan, and Leung designed a linear feedback control law based on the Lyapunov-Krasovskii method for nonlinear systems with singular Jacobian matrixes and applied the control law to chaotic behavior of a disturbed gyrostator [46].

This section will treat controlling chaotic attitude motion of magnetic rigid spacecraft in an elliptic orbit in the gravitational and geomagnetic field. Based on the governing equation of controlled spacecraft, the parametric open-plus-closed-loop method and the stability criterion method will respectively apply to control chaos to a given fixed point or periodic motion and to stabilize chaos to a periodic motion.

5.4.2 Dynamical Model of Controlled Spacecraft

Consider a magnetic rigid spacecraft moving in an elliptic orbit in the gravitational and magnetic field of the Earth. The chaotic attitude motion was treated in Section 3.3.2. However, the spacecraft here has an actuator that can provide the control torque M_c . Then Eq. (3.3.2) becomes

$$\dot{G} = M_g + M_m + M_d + M_c \quad (5.4.1)$$

With the same notations and in a similar way, the dimensionless governing equation of controlled spacecraft can be derived from the projection of Eq. (5.4.1) as

$$\begin{aligned} \ddot{\varphi} - \frac{2e \sin \nu}{1 + e \cos \nu} (1 + \dot{\varphi}) + \frac{\kappa \sin 2\varphi}{1 + e \cos \nu} + \frac{\gamma}{(1 + e \cos \nu)^2} \dot{\varphi} \\ - \alpha \frac{\cos(\varphi + \nu + \omega) - 3 \cos(\varphi - \nu - \omega)}{1 + e \cos \nu} = \frac{u}{(1 + e \cos \nu)^4} \end{aligned} \quad (5.4.2)$$

where

$$u = \frac{p^3}{C\mu} M_c$$

5.4.3 Applications of the Parametric Open-plus-closed-loop Method

Equation (5.4.2) can be cast into the form of Eq. (5.2.12) with

$$f(\varphi, \dot{\varphi}, u, \nu) = \frac{2e \sin \nu}{1 + e \cos \nu} (1 + \dot{\varphi}) - \frac{\kappa \sin 2\varphi}{1 + e \cos \nu} - \frac{\gamma}{(1 + e \cos \nu)^2} \dot{\varphi} + \alpha \frac{\cos(\varphi + \nu + \omega) - 3 \cos(\varphi - \nu - \omega)}{1 + e \cos \nu} + \frac{u}{(1 + e \cos \nu)^4} \quad (5.4.3)$$

It follows that

$$\begin{aligned} f'_\varphi &= \frac{2e \sin \nu}{1 + e \cos \nu} - \frac{\gamma}{(1 + e \cos \nu)^2} \\ f'_\dot{\varphi} &= -\frac{2\kappa \cos 2\varphi}{1 + e \cos \nu} - \alpha \frac{\sin(\varphi + \nu + \omega) - 3 \sin(\varphi - \nu - \omega)}{1 + e \cos \nu} \\ f'_u &= \frac{1}{(1 + e \cos \nu)^4} \end{aligned} \quad (5.4.4)$$

Substitution of Eqs. (5.4.3) and (5.4.4) into Eq. (5.2.13) yields the parametric open-plus-closed-loop control law for the spacecraft.

For the chaotic motions in Eq. (3.4.3) with the parameters given by Eqs. (3.4.16) and (3.4.17), respectively, the control goals successively are taken as a fixed point

$$\varphi_{g1}(\nu) = 0 \quad (5.4.5)$$

and a period-2 motion

$$\varphi_{g2}(\nu) = \sin 0.5\nu \quad (5.4.6)$$

Start control after $\nu_0 = 1300$. Let $\varepsilon = 1.0$, and choose $\alpha = 2.8$ and $\beta = 4.0$ in Eq. (5.2.14). The results for two goals are shown in Figs. 5.20 and 5.21, respectively. The solid lines stand for the libration angle subjected to the parametric open-plus-closed-loop control law (5.2.13). The dashed lines stand for the libration angle subjected to the input-output linearization control law [31]. The dot lines denote the libration angle of the uncontrolled system. In this example, the parametric open-plus-closed-loop control has a slightly longer transition process to achieve the goals.

The control signals $u = u(\nu)$ for φ_{g1} and φ_{g2} are respectively shown in Figs. 5.22 and 5.23. The solid lines stand for the control inputs given by Eq. (5.2.13), and the dashed lines stand for the control inputs of the input-output linearization control law. For both the goal φ_{g1} and φ_{g2} , a great pulse input is needed to activate the input-out linearization control. Since the parametric open-plus-closed-loop

Chaos in Attitude Dynamics of Spacecraft

control begins just when the chaotic phase trajectory is close to the goal periodic orbit, only a small pulse signal is necessary.

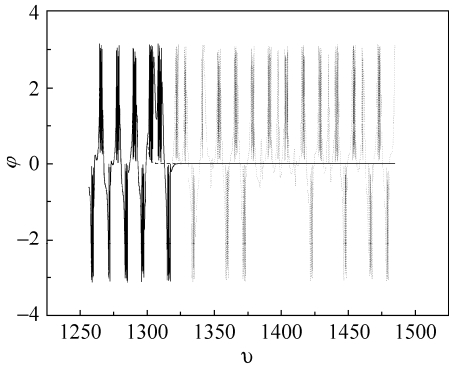


Figure 5.20 Control of chaos to the fixed point

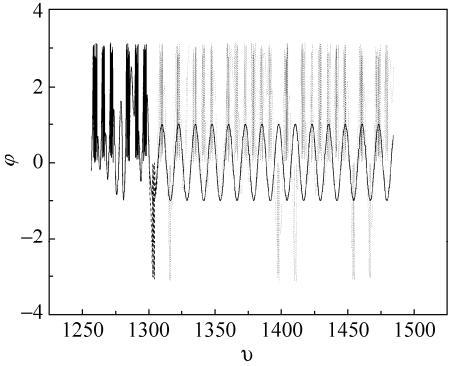


Figure 5.21 Control of chaos to the period-2 motion

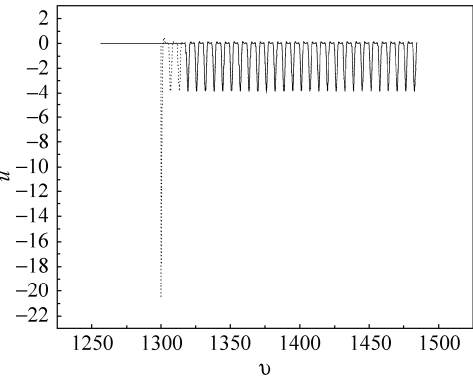


Figure 5.22 Control input for the fixed point

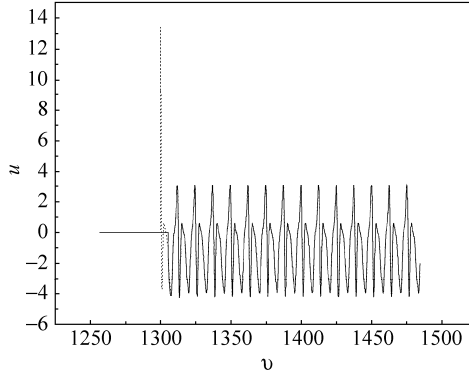


Figure 5.23 Control input for the period-2 motion

5.4.4 Applications of the Stability Criterion Method

Equation (5.4.2) can be rewritten in the form of Eq. (5.2.25) by introducing $x_1 = \varphi$ and $x_2 = d\varphi/d\nu$,

$$\begin{aligned}\dot{x}_1 &= f_1(x_1, x_2, \nu) + u_1 \\ \dot{x}_2 &= f_2(x_1, x_2, \nu) + u_2\end{aligned}\quad (5.4.7)$$

where

$$\begin{aligned}f_1(x_1, x_2, \nu) &= x_2 \\ f_2(x_1, x_2, \nu) &= \frac{2e \sin \nu}{1 + e \cos \nu} (1 + \varphi) - \frac{\kappa \sin 2\varphi}{1 + e \cos \nu} - \frac{\gamma}{(1 + e \cos \nu)^2} \dot{\varphi} \\ &\quad + \alpha \frac{\cos(\varphi + \nu + \omega) - 3 \cos(\varphi - \nu - \omega)}{1 + e \cos \nu}\end{aligned}\quad (5.4.8)$$

$$u_2 = \frac{u}{(1 + e \cos \nu)^4}$$

and u_1 is an additional control input.

The nonlinear vector function

$$\mathbf{f}(\mathbf{x}, \nu) = \begin{pmatrix} x_2 \\ f_2(x_1, x_2, \nu) \end{pmatrix}\quad (5.4.9)$$

can be cast into Eq. (5.3.1) with

$$\mathbf{A} = \begin{pmatrix} -0.5 & 1 \\ 0 & -0.5 \end{pmatrix}, \quad \mathbf{h}(\mathbf{x}, t) = \begin{pmatrix} 0.5x_1 \\ f_2(x_1, x_2, \nu) + 0.5x_2 \end{pmatrix}\quad (5.4.10)$$

where matrix \mathbf{A} has double negative real eigenvalues -0.5 satisfying the stability

condition of linear system (5.3.6). The stability criterion method control law to stabilize goal $\mathbf{x}_g(t)$ is derived from Eq. (5.3.7)

$$\mathbf{u} = \begin{cases} \begin{pmatrix} -0.5x_1 + 0.5x_{g1} \\ -f_2(x_1, x_2, \nu) - 0.5x_2 + f_2(x_{g1}, x_{g2}, \nu) + 0.5x_{g2} \end{pmatrix} & \text{if } \|\mathbf{x} - \mathbf{x}_g\| < \varepsilon \\ \mathbf{0} & \text{otherwise} \end{cases} \quad (5.4.11)$$

For uncontrolled case with parameters given by Eq. (3.4.18), the chaotic motion occurs. The stability criterion method will be applied to stabilize the chaotic motion onto the period-1 trajectory as a fixed point in the Poincaré map. The fixed point is approximately estimated at $(0.50237, 0.74536)^T$. The results of stabilization of the unstable period-1 orbit with $\varepsilon = 0.06$ are shown in Fig. 5.24, where i is the step of data sampling and δ is the error between the presently sampled point and its previous point, namely,

$$\delta = \|\mathbf{x}(iT) - \mathbf{x}((i-1)T)\| \quad (5.4.12)$$

After a transient process, the system comes into periodic region at 31st sampled $\nu = 31T$. The control input is maintained until $\nu = 81T$ and then it is turned off. The stabilization process of the period-1 trajectory is shown in Fig. 5.24(a). The

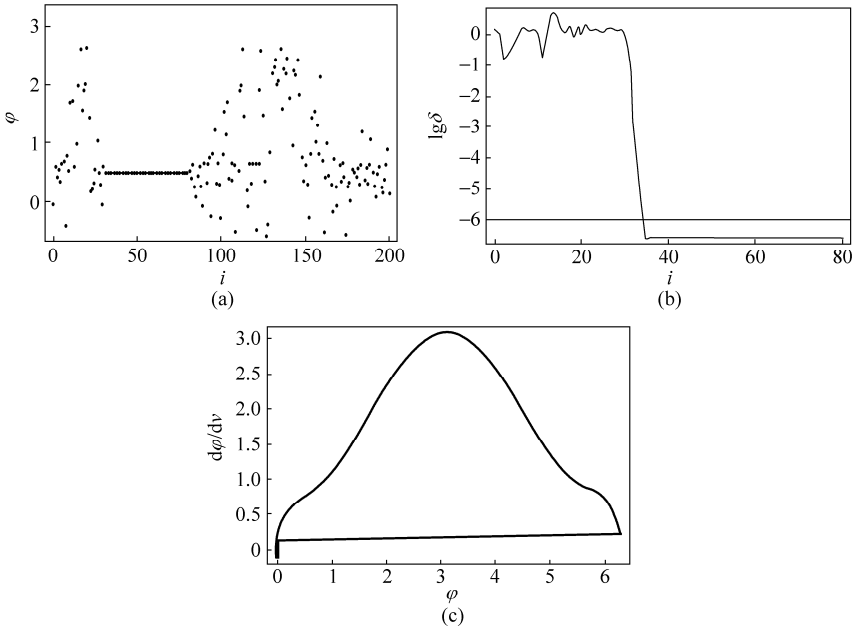


Figure 5.24 Results of stabilization of the unstable period-1 orbit with $\varepsilon = 0.06$: (a) stabilization process of period-1 orbit, (b) the plot of $\lg \delta$ versus i and (c) the period-1 orbit

error δ rapidly decreases with each step and eventually becomes less than 10^{-6} signifying that the period-1 orbit is automatically detected in the control process with increasing accuracy. The fast convergence property is shown in Fig. 5.24(b). The detected period-1 orbit is plotted in the phase plane as shown in Fig. 5.24(c), which is embedded within the chaotic attractor.

The magnitude of control input $u = |\mathbf{u}|$ for stabilization of period-1 orbit is shown in Fig. 5.25. In the transient process, u is rather large in the case of $\varepsilon = 1.5$ (Fig. 5.25(c)), and is sufficient small in the case of $\varepsilon = 0.06$ (Fig. 5.25(a)). The control is switched on only when the trajectory comes near the period-1 orbit at certain time, namely, when the condition of $\varepsilon < 0.06$ is satisfied.

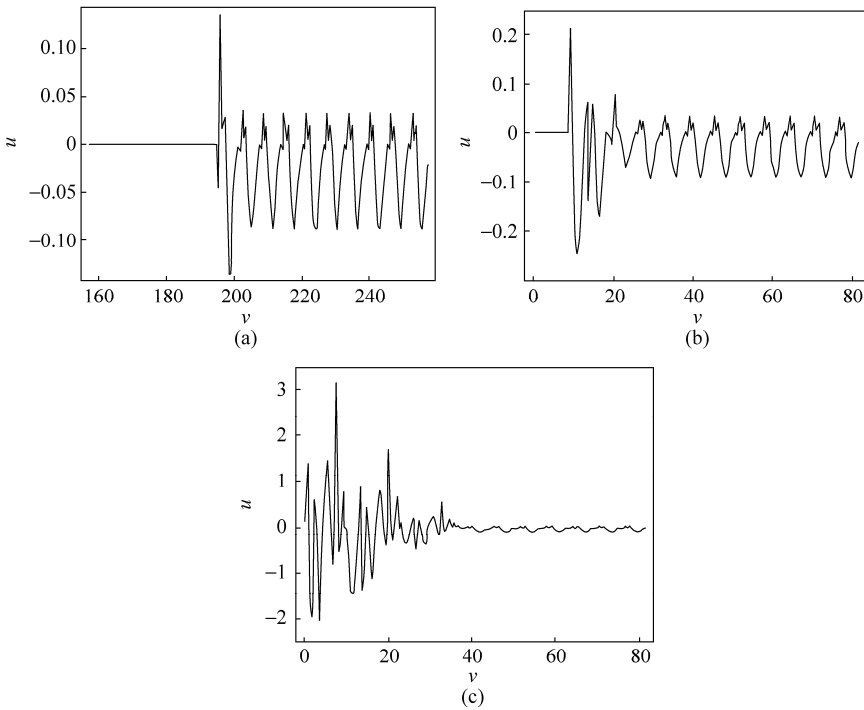


Figure 5.25 The control input $u(\nu)$, (a) $\varepsilon = 0.06$; (b) $\varepsilon = 0.3$ and (c) $\varepsilon = 1.5$

The influence of restriction value ε on the convergence speed of the control process is illustrated in Fig. 5.26. The shortest control steps i_{\min} is defined as the step at which the error δ becomes 10^{-6} . It is shown in Fig. 5.26 that, if ε is larger than 0.26, the convergence of control is quite fast ($7 < i_{\min} < 10$). The shortest control steps i_{\min} fluctuate between 6 and 65 for $0.04 < \varepsilon < 0.25$. Hence, an appropriate value of ε can be chosen to suit different control requirements.

The results of the flexible control of the chaos to unstable period-1 or period-2

Chaos in Attitude Dynamics of Spacecraft

orbits are shown in Fig. 5.27. The control is turned on at the 20th step after free running, and the chaos is stabilized on period-1 orbit. After the maintenance of the control for 50 steps, the orbit returns to chaos as the control is turned off. The control is turned on again to stabilize the period-2 orbit at the 100th step, and then lasts for 60 steps.

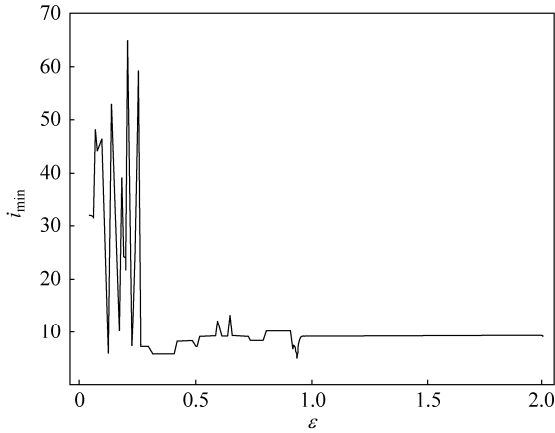


Figure 5.26 Influence of ε on shortest control steps i_{\min}

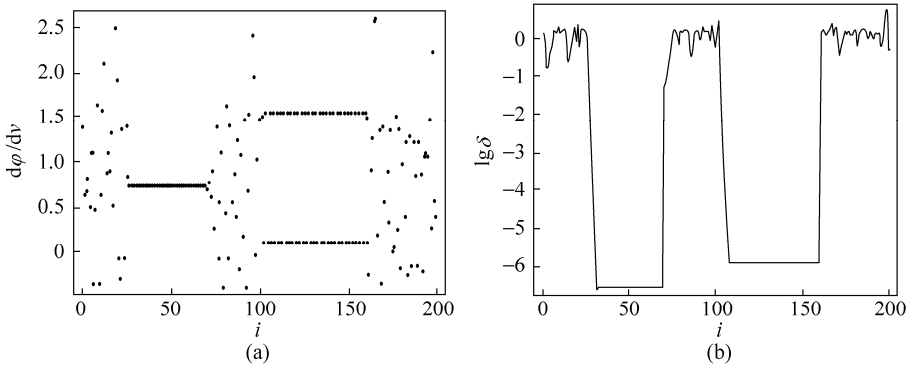


Figure 5.27 Flexible control of the chaotic attitude motion: (a) process of stabilization of period-1 and period-2 orbits, and (b) the plot of $\lg \delta$ versus i

References

- [1] Ott E, Grebogi C, Yorke JA. Controlling chaos. *Physical Review Letters*, 1990, 64, 1196-1199
- [2] Slotine JJE, Li W. *Applied Nonlinear Control*. Englewood Cliffs: Prentice-Hall, 1991

- [3] Auerbach D, Grebogi C, Ott E, Yorke JA. Controlling chaos in high dimensional systems. *Physical Review Letters*, 1992, 69, 3479-3482
- [4] Ogata K. *Modern Control Engineering* (4th edn.). Englewood Cliffs: Prentice-Hall, 2002
- [5] Boccaletti S, Kurths J, Osipov G, Valladares DL, Zhou CS. *The synchronization of chaotic systems. Physics Reports*, 2002, 366, 1-101
- [6] Chen LQ. A general formalism for synchronization in finite dimensional dynamical systems. *Chaos, Solitons and Fractals*, 2004, 19(5), 1239-1242
- [7] Jackson EA. The entrainment and migration controls of multiple-attractor systems. *Physics Letters A*, 1990, volume 151(9), 478-484
- [8] Hübler AW, Lüscher E. Resonant stimulation and control of nonlinear oscillator. *Naturwissenschaft*, 1989, 76, 67-69
- [9] Jackson EA. On the control of complex dynamic systems. *Physica D*, 1991, 50, 341-366
- [10] Jackson EA. Controls of dynamic flows with attractors. *Physical Reviews A*, 1991, 44, 4839-4853
- [11] Mettin R, Hübler A, Scheeline A, Lauterborn W. Parametric entrainment control of chaotic systems. *Physical Reviews E*, 1995, 51, 4065-4075
- [12] Jackson EA, Grosu I. An open-plus-closed-loop (OPCL) control of complex dynamic systems. *Physica D*, 1995, 85, 1-9
- [13] Jackson EA. The OPCL method of entrainment, model-resonance, and migration actions applied to multiple-attractor systems. *Chaos*, 1997, 7, 550-559
- [14] Chen LQ, Liu YZ. A modified open-plus-closed-loop control of chaos in nonlinear oscillations. *Physics Letters A*, 1998, 245(1-2), 87-90
- [15] Chen LQ, Liu YZ. A parametric open-plus-closed-loop approach to control chaos in nonlinear oscillations. *Physics Letters A*, 1999, 262, 350-357
- [16] Yu HJ, Liu YZ, Peng JH. Continuous control of chaos based on the stability criterion. *Physical review E*, 2004, 69, 066203
- [17] Pyragas K. Continuous control of chaos by self-controlling feedback. *Physics Letters A*, 1992, 170, 421-428
- [18] Ushio T. Chaotic synchronization and controlling chaos based on contraction mappings. *Physics Letters A*, 1995, 198, 14-22
- [19] Roy R, Murphy TW, Majer TD, Gills Z, Hunt E. Dynamical control of a chaotic laser: experimental stabilization of a globally coupled system. *Physical Review Letters*, 1992, 68, 1255-1258
- [20] Yu HJ, Liu YZ. Chaotic synchronization based on stability criterion of linear systems. *Physics Letters A*, 2003, 314, 293-298
- [21] Shinbrot T, Grebogi C, Ott E, Yorke JA. Using small perturbations to control chaos. *Nature*, 1993, 363, 411-417
- [22] Xu D, Bishop SR. Self-locating control of chaotic systems using Newton algorithm. *Physics Letters A*, 1996, 210, 273-278
- [23] Dracopoulos DC, Jones AJ. Neuro-genetic adaptive attitude control. *Neural Computing & Applications*, 1994, 2, 183-204
- [24] Dracopoulos DC, Jones AJ. Neural networks and genetic algorithms for the attitude control problem, *Lecture Notes in Computer Science*, 1995, 930, 315-321

Chaos in Attitude Dynamics of Spacecraft

- [25] Dracopoulos DC, Jones AJ. Adaptive neuro-genetic control of chaos applied to the attitude control problem, *Neural Computing & Applications*, 1997, 6(2), 102-115
- [26] Sinha S, Ramaswamy R, Rao JS. Adaptive control in nonlinear dynamics. *Physica D*, 1991, 43, 118-128
- [27] Rollins RW, Parmananda P, Sherard P. Controlling chaos in highly dissipative systems: a simple recursive algorithm. *Physical Review E*, 1996, 47, R780-783
- [28] Meehan PA, Asokanathan SF. Control of chaotic motion in a spinning spacecraft with a circumferential nutational damper. *Nonlinear Dynamics*, 1998, 17(3), 269-284
- [29] Iñárrrea M, Lanchares V, Salas JP, Spin rotor stabilization of a dual-spin spacecraft with time dependent moments of inertia, *International Journal of Bifurcation and Chaos*, 1998, 8(3), 609-617
- [30] Chen LQ, Liu YZ. Chaotic attitude motion of non-spinning spacecraft and its parametric open-plus-closed-loop control. *Acta Mechanica Sinica*, 1998, 30, 363-369 (in Chinese)
- [31] Chen LQ, Liu YZ. The inversion system control of chaotic oscillations. *Technische Mechanik*, 1999, 19(1), 1-4
- [32] Chen LQ, Liu YZ. Controlling chaotic attitude motion of spacecraft by the input-output linearization. *Zeitschrift für Angewandte Mathematik und Mechanik*, 2000, 80, 701-704
- [33] Fujii HA, Ichiki W, Suda S, Watanabe TR. Chaos analysis in librational control of gravity-gradient satellite in elliptic orbit, *Journal of Guidance, Control, and Dynamics*, 2000, 23(1), 145-146
- [34] Oliveira AG, Jones AJ. Synchronization of chaotic trajectories using parameter control. *Proceedings of the 1st International Conference of Control of Oscillators and Chaos* (eds. Chernousko FL, Fradkov AL), 1997, 1, 46-49
- [35] Ding M, Yang W, In V, Ditto WL, Spano ML, Gluckman B. Controlling chaos in high dimensions: theory and experiment. *Physical Reviews E*, 1996, 53, 4334-4344
- [36] Tsui APM, Jones AJ. The control of higher dimensional chaos: comparative results for the chaotic satellite attitude control problem, *Physica D*, 2000, 135, 41-62
- [37] Bernhard B, Hans T. A simple strategy for the deployment of a tethered satellite system. *Zeitschrift für Angewandte Mathematik und Mechanik*, 2001, 81, S177-S178
- [38] Meehan PA, Asokanathan SF. Control of chaotic motion in a dual-spin spacecraft with nutational damping. *Journal of Guidance, Control, and Dynamics*, 2002, 25(2), 209-214
- [39] Meehan PA, Asokanathan SF. Control of chaotic instability in a dual-spin spacecraft with dissipation using energy methods. *Multibody System Dynamics*, 2002, 7, 171-188
- [40] Meehan PA, Asokanathan SF. Control of chaotic instabilities in a spinning spacecraft with dissipation using Lyapunov's method. *Chaos, Solitons and Fractals*, 2002, 13(9), 1857-1869
- [41] Chen LQ, Liu YZ. A modified exact linearization control for chaotic oscillators. *Nonlinear Dynamics*, 1999, 20, 309-317
- [42] Kojima H, Iwasaki M, Fujii HA, Blanksby C, Trivailo P. Nonlinear control of librational motion of tethered satellites in elliptic orbits, *Journal of Guidance, Control, and Dynamics*, 2004, 27(2), 229-239
- [43] Yu HJ, Liu YZ. Control of chaotic attitude motion of a magnetic spacecraft in a complex force field. *Journal of Shanghai Jiao Tong University*, 2004, 38(8), 1408-1411 (in Chinese)

- [44] Liu YZ, Yu HJ, Chen LQ. Chaotic attitude motion and its control of spacecraft in elliptic orbit and geomagnetic field. *Acta Astronautica*, 2004, 55(3-9), 501-508
- [45] Barkow B, Steindl A, Troger H. A targeting strategy for the deployment of a tethered satellite system. *IMA Journal of Applied Mathematics*, 2005, 70, 626-644
- [46] Kuang JL, Meehan PA, Leung AYT. Suppression chaos via Lyapunov-Krasovskii's method. *Chaos, Solitons and Fractals*, 2006, 27, 1408-1414
- [47] Chen LQ and Liu YZ. Chaotic attitude motion of a magnetic rigid spacecraft and its control. *International Journal of Non-Linear Mechanics*, 2002, 37(3), 493-504
- [48] Liu YZ, Chen LQ. Chaotic attitude motion of a magnetic rigid spacecraft in an elliptic orbit and its control, *Acta Mechanica Sinica*, Year???, 19(1), 71-78
- [49] Ge ZM, Lee CI, Chen HH, Lee SC. Nonlinear dynamics and chaos control of a damped satellite with partially-filled liquid, *Journal of sound and Vibration*, 1998, 217, 807-825
- [50] Nayfeh AH, Balachandran B. *Applied Nonlinear Dynamics: Analytical, Computational, and Experiment Methods*. New York: John Wiley & Sons, 1995
- [51] Swinney HL, Gollub JP. The transition to turbulence. *Physics Today*, 1978, 31, 41-49